Retrocrural Lymph Node Metastasis Disclosed by ^{18}F-FDG PET/CT: A Predictor of Supra-diaphragmatic Spread in Ovarian Cancer

Hyung-Jun Im · Yong-il Kim · Jin Chul Paeng · June-Key Chung · Soon-Beom Kang · Dong Soo Lee

Abstract

Purpose Retrocrural lymph nodes (RCLNs) communicate with retroperitoneal and posterior mediastinal LNs. It is possible that, when RCLNs are involved, supra-diaphragmatic extension will occur in abdomino-pelvic cancers. The authors investigated performance of ^{18}F-FDG PET/CT to diagnose RCLN metastasis and whether RCLN metastases were associated with supra-diaphragmatic lymphatic metastases of ovarian cancer.

Materials and methods Sixty-seven patients with stage IV ovarian cancer who had undergone ^{18}F-FDG PET/CT were included in this retrospective study. Diagnostic performance of ^{18}F-FDG PET/CT for RCLN metastasis was evaluated. Patients were divided into two groups by presence or absence of supra-diaphragmatic LN metastasis. The prevalences of RCLN metastasis between the two groups were compared and the odds ratio was calculated.

Results Sensitivity and specificity of ^{18}F-FDG PET/CT for RCLN metastasis were 96.3 and 100%, respectively. Of the 67 study subjects, 27 patients had RCLN metastases (40.3%). Fifty patients had supra-diaphragmatic LN metastases. ^{18}F-FDG PET/CT showed 26 RCLN metastases in patients with supra-diaphragmatic LN metastases (54.5%), and only 1 in patients without supra-diaphragmatic LN metastasis (5.9%), and the difference between two groups was statistically significant ($P<0.05$). The odds ratio that patients with RCLN metastasis would have supra-diaphragmatic LN metastasis was 17.3 (95% confidence interval=2.1 to 140.9, $P=0.008$).

Conclusion Performance of ^{18}F-FDG PET/CT to diagnose RCLN metastasis was excellent. RCLN metastasis revealed by ^{18}F-FDG PET/CT was strongly associated with supra-diaphragmatic LN spread of ovarian cancer. Thus, RCLN metastasis could be used as a predictor of supra-diaphragmatic lymphatic metastasis of ovarian cancer.

Keywords F-FDG · PET/CT · Ovarian cancer · Retrocrural lymph node · Lymphatic metastasis

H.-J. Im · Y.-i. Kim · J. C. Paeng · J.-K. Chung · D. S. Lee
Department of Nuclear Medicine,
Seoul National University College of Medicine,
Seoul, Korea

J.-K. Chung
Cancer Research Institute,
Seoul National University College of Medicine,
Seoul, Korea

J.-K. Chung · D. S. Lee
Institute of Radiation Medicine,
Seoul National University College of Medicine,
Seoul, Korea

S.-B. Kang
Department of Obstetrics and Gynecology,
Seoul National University College of Medicine,
Seoul, Korea

H.-J. Im · Y.-i. Kim · D. S. Lee
Department of Molecular Medicine and Biopharmaceutical
Sciences, WCU Graduate School of Convergence Science and
Technology, Seoul National University,
Seoul, Korea

J.-K. Chung (✉)
28, Yeongeon-dong, Jongno-gu,
Seoul 110-799, Korea
e-mail: jkchung@snu.ac.kr

Introduction

Ovarian cancer has the highest mortality rate among gynecological malignancies in the United States [1] and

the second highest in South Korea [2]. This is attributed to the fact that the majority of ovarian cancer cases are diagnosed in the advanced stage. The Surveillance, Epidemiology, and End Results (SEER) cancer statistics show that 62% of ovarian cancer patients are diagnosed after the disease has metastasized and that the 5-year relative survival rates of ovarian cancer are 93.5% for localized disease and 27.6% for metastatic disease [3].

Distant metastatic disease in ovarian cancer can be divided into two categories according to the 7th edition of the *American Joint Committee on Cancer Staging Manual* [4]. One is metastasis to distant organs such as the liver parenchyma, lung, bone, and brain. The other is metastasis to extra-abdominal lymph nodes. Thus detecting extra-abdominal, usually supra-diaphragmatic, lymph node metastasis is important for accurate staging and predicting prognosis.

The retrocrural space (RCS) is a small triangular area within the most inferior posterior mediastinum and is bordered by two diaphragmatic crura. This area includes the aorta, the azygos and hemiazygos veins, nerves, thoracic duct, and lymph nodes, which are called the retrocrural lymph nodes [5]. Retrocrural lymph nodes (RCLNs) receive lymph from the posterior part of the diaphragm and communicate with the posterior mediastinal nodes and para-aortic nodes in the upper abdomen [6] (Fig. 1). In view of their locations, it is possible that when RCLNs are involved, supra-diaphragmatic lymph node metastasis could occur in cases of abdomino-pelvic cancer. However, no study has yet supported this possibility in abdomino-pelvic cancer despite its suggestion in some case reports [7, 8].

The advent of positron emission tomography (PET) and its later refinements have increased our appreciation of lymphatic metastasis patterns in various cancers. In fact, the determination of lymphatic involvement in the whole body can be more easily and accurately evaluated by ^{18}F-FDG PET than by any other conventional modality (including CT, MR, and lymphangiography). However, although ^{18}F-FDG PET has proven utility in many cancer types, only rarely has it been used to evaluate patterns of lymphatic spread.

The present study was to investigate performances of ^{18}F-FDG PET and contrast-enhanced CT to diagnose RCLN metastasis, to determine whether RCLN metastasis was associated with supra-diaphragmatic lymphatic metastases, and to observe the prevalence of metastasis to each involved organ and LN-bearing site in stage IV ovarian cancer.

Materials and Methods

Patients

From 2007 to 2009, 760 patients with ovarian cancer underwent ^{18}F-FDG PET/CT in our institute. Of these, 82
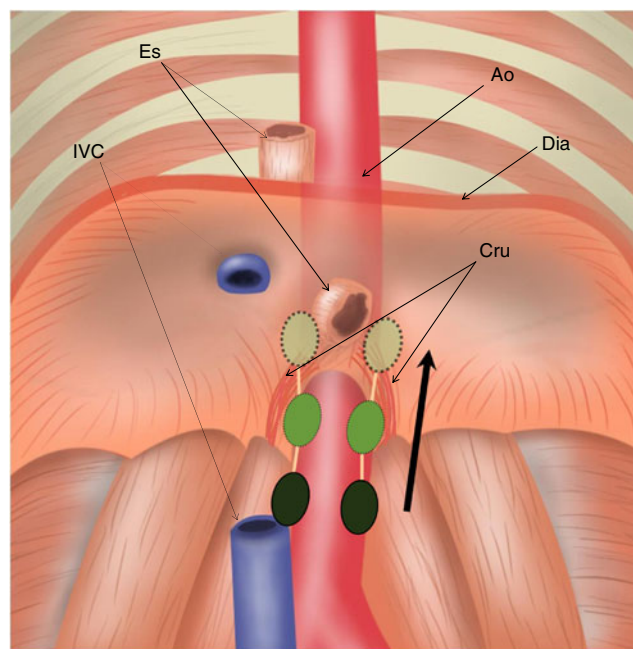

Fig. 1 Location and lymphatic communication of RCLNs. Diagram of RCLNs (*green*) located in retrocrural space. RCLNs communicate with posterior mediastinal LNs (*light green with dotted line*) and para-aortic LNs (*dark green*) in the upper abdomen. *Ao* Aorta, *IVC* inferior vena cava, *Es* esophagus, *Dia* diaphragm, *Cru* diaphragmatic crura, *RCLN* retrocrural LN

had evidence of distant metastatic lesions by ^{18}F-FDG PET/CT with increased CA-125 level (mean±SD; 1,269± 2,364.8) at least once during the follow-up period. In this study, 8 of the 82 were excluded because distant metastatic lesions were not confirmed by either biopsy or other imaging, and another 7 were excluded because of the presence of a concomitant second primary malignancy. Finally, 67 patients with stage IV ovarian cancer were evaluated in the present study (mean age 55.6 years, range 31~80 years). Indications for PET/CT scanning were initial staging (*n*=28) and restaging (*n*=39). The study was approved by the Institutional Review Board for review of medical records of the patients. Histopathologic types of primary lesions of these patients were confirmed by cytoreductive surgery in 61 patients. The histopathologic types were 40 serous cystadenocarcinoma, 6 mucinous cystadenocarcinoma, 4 endometrioid adenocarcinoma, 3 clear cystadenocarcinoma, 5 undifferentiated carcinoma, 1 mucinous tumor of borderline malignancy, 1 transitional cell carcinoma, and 1 mixed epithelial tumor. Histopathologic types of the other six patients were not identified because they did not undergo cytoreductive surgery, however they were initially diagnosed as ovarian cancer by radiological findings (e.g., large cystic and solid ovarian mass with ascites) and increased serum CA-125 level (mean±SD; 1,241.5±2,427.5, range 49.5~6,350), and ascites cytology (metastatic adenocarcinoma). For the

analysis, the patients were divided into two groups according to presence or absence of supra-diaphragmatic LN metastasis (Table 1).

^{18}F-FDG PET/CT Protocol

^{18}F-FDG PET/CT was performed using a PET/CT scanner (Biograph 40 Truepoint with TRUE V; Siemens Medical Solutions, Hoffman Estates, IL). After fasting for at least 6 h, the patients were injected intravenously with 5.2 MBq of ^{18}F-FDG per kilogram of body weight. PET/CT scanning was performed from the middle of the skull to the upper thigh at 60 min after injection. During the PET/CT scans, spiral CT was performed using the following parameters: a scout view at 30 mA and 120 kVp, followed by a spiral CT scan with an effective mA of 50, 120 kVp, a 5 mm section width, 4 mm collimation, 12 mm table feed per rotation, and 0.8 s per rotation with the arms raised. The PET images were acquired after the CT scans at 2 min per each bed position [21.6 cm increments (three-dimensional mode)].

The PET images were reconstructed onto a matrix of 128×128 using the ordered-subsets expectation maximization algorithm (four iterations and eight subsets), and attenuation correction was also performed. The CT images were reconstructed onto a 512×512 matrix, and they were converted using 511-keV-equivalent attenuation factors for the attenuation correction. The PET, PET/CT, and CT

Table 1 Patient characteristics

Characteristics	Values
Number of patients	67
Mean age	55.6±10.6 years
Age range	31–80 years
Histopathologic type	
Serous cystadenocarcinoma	40 (59%)
Mucinous cystadenocarcinoma	6 (9%)
Endometrioid adenocarcinoma	4 (6%)
Clear cell cystadenocarcinoma	3 (4%)
Undifferentiated carcinoma	5 (7%)
Other[a]	3
Not assessable	6
Confirmation of distant metastasis	
Biopsy	7 (10%)
Supraclavicular LN metastasis	5
Lung metastasis	2
Image review	60 (90%)
Supra-diaphragmatic LN metastasis	
Presence	50 (75%)
Absence	17 (25%)

[a] Mucinous tumor of borderline malignancy, transient cell carcinoma, mixed epithelial tumor

images were reviewed using a dedicated workstation and software (E.soft; Siemens Medical Solutions), which allowed 3-D displays (transaxial, coronal, and sagittal) to be constructed using the CT, PET, and PET/CT images and the maximum intensity projection displays of the PET data.

To quantify ^{18}F-FDG uptakes, standardized uptake values (SUV) were calculated as follows: SUV=[decay-corrected activity (kBq) per mL of tissue volume/injected ^{18}F-FDG activity (kBq) per body mass (g)]. The SUV of a lesion was obtained by placing regions of interest (ROIs) manually around the lesion, and the maximum SUV (SUVmax) within an ROI was used to minimize partial-volume effects.

Image Evaluation and Confirmation of Metastasis

^{18}F-FDG PET/CT images were evaluated by consensus between two nuclear medicine physicians (H.J.I, J.K.C). When patient had undergone an ^{18}F-FDG PET/CT scan more than once, we selected the scan that first showed evidence of distant metastasis.

Firstly, a lesion was considered as suspected metastasis on ^{18}F-FDG PET/CT scan if its metabolic activity was greater than that of surrounding tissue and if it was not associated with a physiologically active organ (urinary system, bowel, stomach, heart, or another) by visual analysis. Next, on quantitative analysis, an SUVmax value greater than 2.5 (3.5 for the liver) was taken to support a suspicion of metastasis [9, 10]. Suspicious metastatic lesions on ^{18}F-FDG PET/CT scan were confirmed by biopsy in 7 patients and by concurrence with contrast-enhanced CT (CECT) and image follow-up in 60 patients. Seven biopsy-proven stage IV cases comprised five cases of supraclavicular lymph node metastases examined by ultrasonography (US)-guided needle biopsy, and two cases of lung metastases examined by CT-guided percutaneous needle biopsy.

CECT images were taken within 1 month from the ^{18}F-FDG PET/CT without any intervention. The CT images were reviewed by consensus between two different radiologists. Metastasis on CT images was determined based on lesion morphology and pattern of contrast enhancement. For lung metastases, newly developed nodules or nodules with typical findings (e.g., multiple, periphery, lower lobe predominancy) when there was no old image available for comparison were considered metastatic. For liver and spleen metastases, only true parenchymal lesions were recorded and newly developed, single or multiple low density lesions not showing cyst or hemangioma patterns were considered metastatic [11]. For pancreatic metastases, rim or homogenous-enhancing single or multiple newly seen nodular lesions were considered metastatic [12]. For bone metastases, multiple osteolytic bone lesions were

considered metastatic. For adrenal gland metastases, nodular mass with strong enhancement in the early arterial phase was considered metastatic. For lymph node metastases, lymph nodes with a short-axis diameter exceeding 10 mm without calcification in one nodal station were considered metastatic [13, 14].

We measured short diameters of all visualized RCLNs by CECT and their SUVmax by ^{18}F-FDG PET/CT.

To confirm a lesion as a metastasis, we compared all of the considered metastatic lesions and all RCLNs with the following CECT or ^{18}F-FDG PET/CT, which was done after 3–6 months. If the abnormality of a lesion progressed (more than 20% increase in diameter or more than 30% increase in SUVmax) [15, 16], the lesion was confirmed to be a metastasis. If a patient had partial or complete response clinically, the lesion was confirmed to be a metastasis when the abnormality improved (30% decrease in diameter or more than 30% decline in SUVmax) [15, 16].

Statistical Analysis

Statistical analysis was performed by using MedCalc for Windows (MedCalc Software, Belgium), and a $P<0.05$ was considered statistically significant. ROC analysis was done to evaluate diagnostic performance to detect RCLN metastasis and to establish the most feasible cut-off value by ^{18}F-FDG PET/CT and CECT. Cut-off values correspond to the highest average of sensitivity and specificity. Chi-squared test was used to evaluate the difference in prevalence of RCLN metastasis between patients with and without supra-diaphragmatic LN metastasis. The odds ratio of having supra-diaphragmatic LN metastasis was calculated when a patient had RCLN metastasis.

Results

Of the 67 patients with stage IV ovarian cancer, RCLNs were visualized in 38 patients by CECT. The mean size and SUVmax of all visualized RCLNs were 7.4±2.9 mm (range 1.9~15 mm) and 2.7±1.3 (range 0.8~6), respectively. Among all visualized RCLNs in CECT, 29 RCLNs showed focal FDG uptake by PET. Of the 67, 27 RCLNs were confirmed to be metastatic (40.3%). The mean size and SUVmax of metastatic RCLNs were 8.5±2.2 mm (range 6.2~15 mm) and 3.4±1.0 (range 1.6~6), respectively. Diagnostic performances of ^{18}F-FDG PET/CT and CECT to detect RCLN metastasis were evaluated by ROC analysis. Areas under the curve of ^{18}F-FDG PET/CT and CECT were 0.998 and 0.971, respectively. Sensitivity, specificity, positive predictive value, and negative predictive value of ^{18}F-FDG PET/CT were 96.3, 100, 100, and 97.6% at an SUVmax cut-off value of 1.8. Those of CECT were 100, 92.5, 90.0, and 100% at a short diameter cut off value of 6.2 mm. There were three false-positive cases and no false-negative cases with CECT. There was only one false-negative case and no false-positives with ^{18}F-FDG PET/CT.

Supra-diaphragmatic LN metastases were found in 50 patients, and the other 17 patients did not have supra-diaphragmatic LN metastasis but had extraperitoneal solid organ metastases. Twenty-six RCLN metastases were found in patients with supra-diaphragmatic LN metastasis (52%), and only one in patients without supra-diaphragmatic LN metastasis (5.9%) (Table 2). Prevalence of RCLN metastasis in patients with supra-diaphragmatic LN metastasis was significantly higher than that in patients without supra-diaphragmatic LN metastasis ($P=0.003$). The odds ratio of having supra-diaphragmatic LN metastasis in patients with RCLN metastasis was 17.33 with a 95% confidence interval of 2.13–140.86 ($P=0.0076$).

Metastatic sites were assessed in all patients. The prevalences of extraperitoneal metastases were 29.9% (20/67) to liver parenchyma, 16.4% (11/67) to lung, and 11.9% (8/67) to bone. In addition, there was evidence of metastasis to the spleen in two cases, to the adrenal gland in two, to the pancreas in one, to the brain in one, and to soft tissue in one.

The prevalences of metastatic sites were 44.8% (30/67) for mediastinum, 41.8% (28/67) for supraclavicular fossa, 7.5% (5/67) for neck, 13.4% (9/67) for axilla, and 17.9% (12/67) for chest wall LN-bearing areas other than axilla (Table 3).

Discussion

^{18}F-FDG PET/CT is superior to other imaging modalities for detecting metastasis to a lymph node or a distant organ in many types of malignancies [17–20]. The reason for this is that ^{18}F-FDG PET/CT provides functional information about cellular glucose metabolism in addition to morphological information.

Diagnostic performances to detect RCLN metastasis by ^{18}F-FDG PET/CT as well as CECT were quite good.

Table 2 Retrocrural lymph node (RCLN) metastasis rates according to supra-diaphragmatic LN metastasis

| | Supra-diaphragmatic LN | | |
	(+)	(−)	Total
RCLN (+)	26	1	27
RCLN (−)	24	16	40
Total	50	17	67

(+) Positive for metastasis, (−) negative for metastasis

Table 3 Sites of distant metastasis

Site	Number (%)
Organ	
Liver	20 (30%)
Lung	11 (16%)
Bone	8 (12%)
Spleen	2 (3%)
Adrenal gland	2 (3%)
Other sites[a]	3 (4%)
Lymph node	
Mediastinum	30 (45%)
SCN	28 (42%)
Right	6
Left	15
Bilateral	7
Neck	5 (7%)
Right	2
Left	2
Bilateral	1
Axilla	9 (13%)
Right	3
Left	4
Bilateral	2
Chest wall other than axilla[b]	12 (18%)

SCN Supraclavicular lymph node

[a] Pancreas, brain, and subcutaneous tissue

[b] Internal mammary and cardiophrenic lymph nodes

Specificity and positive predictive value tended to be higher in ^{18}F-FDG PET/CT, although there was no statistical significance. There were three false-positive cases in CECT that were true negative by ^{18}F-FDG PET/CT. This advantage of ^{18}F-FDG PET/CT for accurate diagnosis of RCLN metastasis was suggested in a previous case report [21]. There was one false-negative case in ^{18}F-FDG PET/CT with SUVmax of 1.6 and short diameter of 6.8 mm. SUVmax of this LN possibly devalued due to the partial volume effect because of small size. However despite the relatively small sizes of metastatic RCLNs in the present study (range 6.2~15 mm), the cut-off value (SUVmax 1.8) to diagnose RCLN metastasis by ^{18}F-FDG PET/CT was similar to previous studies. In a colorectal cancer study, a lymph node SUVmax of greater than 1.6 was suggested as a criterion for lymph node metastasis [22], and in a recent biliary cancer study, a lymph node SUVmax of greater than 2.0 showed better results for detecting LN metastasis than CT diagnosis [23].

If we consider all visually perceptible focal FDG uptakes in RCS as PET positive, we can enhance sensitivity and NPV of PET/CT from 96.3 and 97.6% to 100 and 100%,

respectively, while sacrificing the specificity and PPV of PET/CT from 100 and 100% to 95 and 93.1%, respectively. In our group, with an SUVmax cutoff of 1.7, there would be two false-positive cases and no false-negative cases.

Cut-off value to detect RCLN metastasis by CECT (6.2 mm) was in accordance with a previous study. Callen et al. [24] reported no definable LNs with a diameter greater than 6 mm in the normal retrocrural space on CT image, and a short diameter of RCLN greater than 6 mm has been considered abnormally enlarged. In the present study, the sizes of three false-positive cases of CECT were 6.8, 7.2, and 8.2 mm respectively. Although RCS is not a common site to have reactive or inflammatory lymphadenopathy, Callen et al. also described 3 benign lymphadenopathies in RCS out of 39 [24].

In the stage IV ovarian cancer patients examined during this study, the prevalence of metastasis to RCLNs was 40.3%. In fact, the prevalence of RCLN metastasis was greater than that of any other single distant metastasis except supraclavicular LN metastasis, whether in an LN-bearing area or an organ. We also found that the prevalence of RCLN metastasis was significantly higher in the presence of supra-diaphragmatic LN metastasis than in its absence. Representative PET/CT image of RCLN metastasis and biopsy-proven supraclavicular LN metastasis is demonstrated in Fig. 2.

In particular, the odds ratio of patients with RCLN metastasis having supra-diaphragmatic LN metastasis was as high as 17.3. This means that if a patient has RCLN metastasis, there is a more than 17 times higher chance of having supra-diaphragmatic LN in stage IV ovarian cancer. This indicates that RCLN metastasis can be a predictor of supra-diaphragmatic LN metastasis. A few investigators have already suggested this possibility [4, 6, 7], but their suggestions were not based on systematic analysis.

As far as we know, only two reports have been issued on RCLN metastasis from abdominal or pelvic tumors. Kawamura et al. [7] found that 4 of 6 patients with RCLN swelling had cervical lymph node swelling in stage II, III testicular cancer, and Mahon and Libshitz [25] reported that, of 50 cases with mediastinal lymph node metastases from infra-diaphragmatic cancers, 19 presented with retro-crural adenopathy. However, in these reports CT was used to evaluate lymph node involvement, and it has been established that CT is inferior to ^{18}F-FDG PET in terms of detecting LN metastasis [26, 27]. The prevalence of RCLN metastasis in these studies was 38–40%. Interestingly, the prevalence of RCLN metastasis was similar to the present study regardless of the different tumor types and stages.

In the literature, the common sites of LN involvement in ovarian cancer are abdomen (47%), mediastinum (29%), and the pelvic area (17%). The common sites of distant organ metastasis are liver (45%), lung (39%), pancreas

Fig. 2 Representative PET/CT image of an ovarian cancer patient with RCLN and supra-diaphragmatic LN metastasis MIP image of ^{18}F-FDG PET (a), transaxial ^{18}F-FDG PET image (b), non-contrast-enhanced CT (c), and rigid fusion image (d) of a patient with left ovarian cancer. The images show a left ovarian mass with increased metabolic activity, multiple hypermetabolic LNs at the retroperitoneal area, and a hypermetabolic LN at the left supraclavicular fossa (arrowhead), but no evidence of distant organ involvement. The hypermetabolic LN in the right retrocrural space had an SUVmax of 3.9 and a short diameter of 12 mm and was considered malignant (arrow). The left supraclavicular LN was proven to be metastatic by ultrasonography-guided needle biopsy
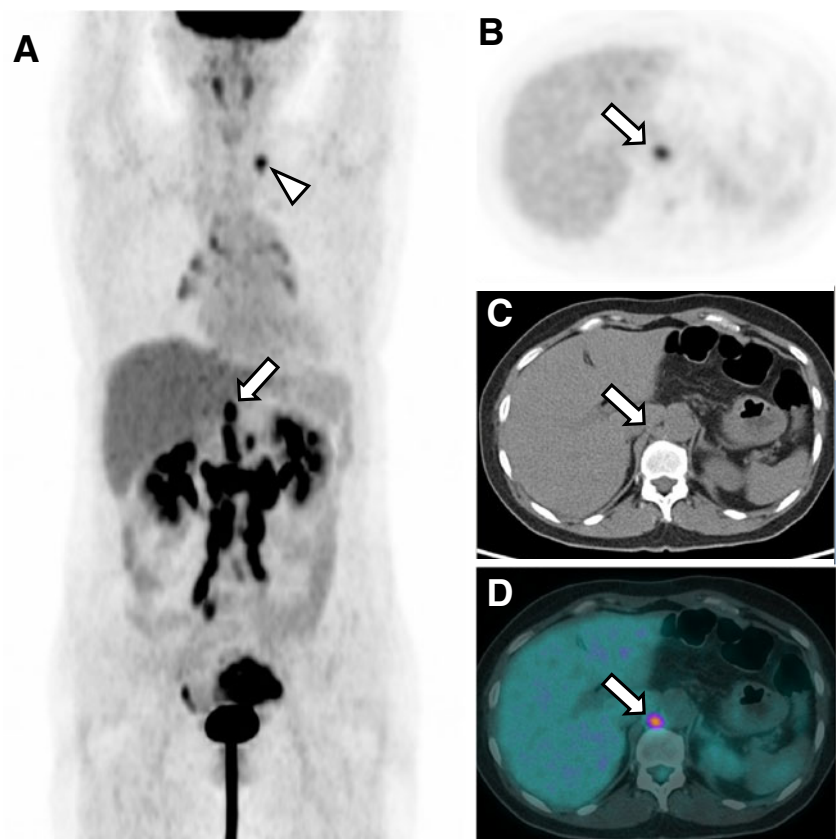
(21%), spleen (15%), bone (11%), kidney (10%), and brain (6%) [28]. Of these sites, we observed metastasis in mediastinal LNs, liver, lung, bone, and brain in our patient group, and the results were similar to the literature.

In the present study, the prevalence of supra-diaphragmatic LN metastasis was particularly high. For example, the prevalence of supraclavicular LN and axillary LN metastasis was 42 and 13%, respectively. In the literature, supra-diaphragmatic LN metastasis is rare in ovarian cancer. Dvoretsky et al. reported that only 4% had metastatic supraclavicular LNs and that no axillary LN metastasis was found in the autopsy results of 100 ovarian cancer patients [28]. We attribute this discrepancy to differences in the cohorts and the analytic methods used. For example, only 18% of Dvoretsky's cohort had stage IV disease, whereas our cohort contained only patients with stage IV disease. Additionally, this discrepancy may be due to the higher survival rates now achieved for ovarian cancer, as Dvoretsky's study was performed in 1988.

The present study has a few limitations. First, metastatic RCLNs were diagnosed only by image analysis because biopsy usually was not possible due to its deep location. However, by image follow-up, we could confirm the diagnosis. Second, although ^{18}F-FDG PET/CT is better than conventional anatomical imaging modalities for detecting lymph node metastasis [26, 27], its ability to detect microscopic metastases is limited. Thus, microscopic metastases missed by ^{18}F-FDG PET/CT could not be included in our observations of patterns of lymphatic spread. Lastly the calculated odds ratio of RCLN metastasis for having supra-diaphragmatic LN metastasis is under-powered because other possible confounding factors were not considered. Thus we expect that further prospective studies with controlled confounding factors will validate the association of RCLN metastasis and supra-diaphragmatic LN metastasis.

Conclusion

Diagnostic performances of RCLN metastasis by ^{18}F-FDG PET/CT and CECT were both quite high without significance difference. The prevalence of RCLN metastasis was significantly higher in patients who had supra-diaphragmatic LN metastases than in patients who did not. Odds ratio of patients with RCLN metastasis having supra-diaphragmatic LN metastasis was as high as 17.3. These findings suggest that RCLN metastasis revealed by ^{18}F-FDG PET/CT is strongly associated with supra-diaphragmatic LN spread of ovarian cancer. Thus, RCLN metastasis revealed by ^{18}F-FDG PET/CT could be used to predict the presence of supra-diaphragmatic lymphatic metastases.

References

1. Jemal A, Siegel R, Ward E, Hao Y, Xu J, Murray T et al. Cancer statistics, 2008. CA Cancer J Clin. 2008;58:71–96.

2. Jung KW, Park SH, Kong HJ, Won YJ, Boo YK, Shin HR et al. Cancer statistics in Korea: incidence, mortality and survival in 2006–2007. J Korean Med Sci. 2010;25:1113–21.

3. Altekruse SF, Kosary CL, Krapcho M, Neyman N, Aminou R, Waldron W et al. SEER cancer statistics review, 1975–2007. National Cancer Institute, Bethesda, MD. http://seer.cancer.gov/csr/1975_2007/, based on November 2009 SEER data submission, posted to the SEER web site, 2010.

4. Edge SB, Byrd DR, Compton CC, Fritz AG, Greene FL, Trotti A, editors. AJCC cancer staging manual, 7th ed. Chicago: American Joint Committee on Cancer; 2009.

5. Restrepo CS, Eraso A, Ocazionez D, Lemos J, Martinez S, Lemos DF. The diaphragmatic crura and retrocrural space: normal imaging appearance, variants, and pathologic conditions. Radiographics. 2008;28:1289–305.

6. Suwatanapongched T, Gierada DS. CT of thoracic lymph nodes. Part I: anatomy and drainage. Br J Radiol. 2006;79:922–8.

7. Shin MS, Berland LL. Computed tomography of retrocrural spaces: normal, anatomic variants, and pathologic conditions. AJR Am J Roentgenol. 1985;145:81–6.

8. Kawamura J, Hida S, Higashi Y, Yamauchi T, Yoshida O. Diagnosis of retroperitoneal lymph node swelling by computed tomography in advanced testicular cancer patients, with special reference to retrocrural lymph node swelling. Hinyokika Kiyo. 1985;31:1105–16.

9. Beggs AD, Hain SF, Curran KM, O'Doherty MJ. FDG-PET as a "metabolic biopsy" tool in non-lung lesions with indeterminate biopsy. Eur J Nucl Med Mol Imaging. 2002;29:542–6.

10. Patz Jr EF, Lowe VJ, Hoffman JM, Paine SS, Burrowes P, Coleman RE et al. Focal pulmonary abnormalities: evaluation with F-18 fluorodeoxyglucose PET scanning. Radiology. 1993;188:487–90.

11. Dauplat J, Hacker NF, Nieberg RK, Berek JS, Rose TP, Sagae S. Distant metastases in epithelial ovarian carcinoma. Cancer. 1987;60:1561–6.

12. Klein KA, Stephens DH, Welch TJ. CT characteristics of metastatic disease of the pancreas. Radiographics. 1998;18:369–78.

13. Webb WR, Gatsonis C, Zerhouni EA, Heelan RT, Glazer GM, Francis IR et al. Radiology. 1991;178:705–13.

14. van den Brekel MW, Stel HV, Castelijns JA, Nauta JJ, van der Waal I, Valk J et al. Cervical lymph node metastasis: assessment of radiologic criteria. Radiology. 1990;177:379–84.

15. Eisenhauer EA, Therasse P, Bogaerts J, Schwartz LH, Sargent D, Ford R et al. New response evaluation criteria in solid tumours: revised RECIST guideline (version 1.1). Eur J Cancer. 2009;45:228–47.

16. Wahl RL, Jacene H, Kasamon Y, Lodge MA. From RECIST to PERCIST: evolving considerations for PET response criteria in solid tumors. J Nucl Med. 2009;50:122S–50S.

17. Liu FY, Lin CY, Chang JT, Ng SH, Chin SC, Wang HM et al. ^{18}F-FDG PET can replace conventional work-up in primary M staging of nonkeratinizing nasopharyngeal carcinoma. J Nucl Med. 2007;48:1614–9.

18. Hubner KF, McDonald TW, Niethammer JG, Smith GT, Gould HR, Buonocore E. Assessment of primary and metastatic ovarian cancer by positron emission tomography (PET) using 2-[^{18}F]deoxyglucose (2-[^{18}F]FDG). Gynecol Oncol. 1993;51:197–204.

19. Tran BN, Grigsby PW, Dehdashti F, Herzog TJ, Siegel BA. Occult supraclavicular lymph node metastasis identified by FDG-PET in patients with carcinoma of the uterine cervix. Gynecol Oncol. 2003;90:572–6.

20. Gontier E, Wartski M, Guinebretiere JM, Alberini JL. ^{18}F-FDG PET/CT in a patient with lymph node metastasis from ovarian adenocarcinoma. AJR Am J Roentgenol. 2006;187:W285–9.

21. Burns N, Barksdale J, Ho L, Colletti PM. Imaging of the cisterna chyli on PET-CT in patients with known malignancy: Report of two cases. Radiol Case Rep. 2009;4:269.

22. Tsunoda Y, Ito M, Fujii H, Kuwano H, Saito N. Preoperative diagnosis of lymph node metastases of colorectal cancer by FDG-PET/CT. Jpn J Clin Oncol. 2008;38:347–53.

23. Kobayashi S, Nagano H, Hoshino H, Wada H, Marubashi S, Eguchi H et al. Diagnostic value of FDG-PET for lymph node metastasis and outcome of surgery for biliary cancer. J Surg Oncol. 2011;103(3):223–9. doi:10.1002/jso.21811

24. Callen PW, Korobkin M, Isherwood I. Computed tomographic evaluation of the retrocrural prevertebral space. AJR Am J Roentgenol. 1977;129:907–10.

25. Mahon TG, Libshitz HI. Mediastinal metastases of infradiaphragmatic malignancies. Eur J Radiol. 1992;15:130–4.

26. Kitajima K, Murakami K, Yamasaki E, Fukasawa I, Inaba N, Kaji Y et al. Accuracy of ^{18}F-FDG PET/CT in detecting pelvic and paraaortic lymph node metastasis in patients with endometrial cancer. AJR AM J Roentgenol. 2008;190:1652–8.

27. Adams S, Baum RP, Stuckensen T, Bitter K, Hor G. Prospective comparison of 18 F-FDG PET with conventional imaging modalities (CT, MRI, US) in lymph node staging of head and neck cancer. Eur J Nucl Med. 1998;25:1255–60.

28. Dvoretsky PM, Richards KA, Angel C, Rabinowitz L, Stoler MH, Beecham JB et al. Distribution of disease at autopsy in 100 women with ovarian cancer. Hum Pathol. 1988;19:57–63.